PNAS RESEARCH ARTICLE | PSYCHOLOGICAL AND COGNITIVE SCIENCES OPEN ACCESS

Brain tract structure predicts relapse to stimulant drug use

Loreen Tisdall[a,b,1], Kelly H. MacNiven[b], Claudia B. Padula[c], Josiah K. Leong[d], and Brian Knutson[b]

Edited by Ranulfo Romo, Universidad Nacional Autonoma de Mexico, Mexico City, D.F., Mexico; received September 10, 2021; accepted May 6, 2022

Diffusion tractography allows identification and measurement of structural tracts in the human brain previously associated with motivated behavior in animal models. Recent findings indicate that the structural properties of a tract connecting the midbrain to nucleus accumbens (NAcc) are associated with a diagnosis of stimulant use disorder (SUD), but not relapse. In this preregistered study, we used diffusion tractography in a sample of patients treated for SUD ($n = 60$) to determine whether qualities of tracts projecting from medial prefrontal, anterior insular, and amygdalar cortices to NAcc might instead foreshadow relapse. As predicted, reduced diffusion metrics of a tract projecting from the right anterior insula to the NAcc were associated with subsequent relapse to stimulant use, but not with previous diagnosis. These findings highlight a structural target for predicting relapse to stimulant use and further suggest that distinct connections to the NAcc may confer risk for relapse versus diagnosis.

diffusion | addiction | relapse | accumbens | insula

Significance

Relapse to addiction presents a global burden for individuals and societies alike, yet the biological mechanisms underlying relapse remain to be determined. We combined diffusion-weighted imaging with tractography to examine the role of brain structure in predicting relapse to stimulant drug use. Reduced diffusion metrics of a tract projecting from the right anterior insula to the nucleus accumbens (NAcc) predicted relapse to stimulant use 6 mo posttreatment but were not associated with previous stimulant use disorder diagnosis. Our findings reveal a structural target for predicting stimulant drug relapse and specifically suggest that, although midbrain connections to the NAcc may be associated with stimulant use disorder diagnosis, cortical connections to the NAcc may instead predict relapse to stimulant use.

Around the world during the year 2020, over 250 million people reported using drugs for nonmedical purposes, with 35.6 million conceding problematic use of drugs (1). Problematic drug use imposes a significant burden on individuals and societies alike by exacting substantial and lasting physical, psychological, economic, and social costs (2). Successful treatments are elusive and relapse remains prevalent (3, 4). Relapse rates vary as a function of substance type (5) but are particularly problematic in the case of stimulant use disorder (SUD) (6) (including [meth]amphetamine and [crack] cocaine). For instance, estimates indicate that ∼50% of methamphetamine users relapse within 6 mo and over 60% relapse within 12 mo after release from treatment (7). Consistent with these estimates, we previously found that 36% of SUD patients relapsed within 3 mo after release from treatment (8). Recent trends in drug use increase the urgency of addressing SUD. While cocaine remains a default choice of drug in the United States, use of stimulants like amphetamines increased by 40% from 2016 to 2018, coinciding with a surge in drug treatment admissions with amphetamine-type stimulants being the primary drug of concern (1). Research into key factors that contribute to relapse to stimulant use might reveal novel targets for prediction, intervention, and treatment.

Predicting drug relapse represents an important first step toward developing better interventions for prevention, but very few measures reliably predict relapse to stimulant use (9). While many physiological, psychological, social, and clinical factors have been associated with the risk of relapse across a broad range of substances (3, 5), the role of these factors in relapse to stimulant use is less clear. Since addiction has been associated with alterations in neural circuits (10, 11), new neuroimaging methods offer the hope that neural markers related to addiction can be noninvasively measured in humans (12).

Research on animal models has centrally implicated dopaminergic projections from the midbrain in addiction (13, 14). Specifically, dopamine release and activation of receptors in the nucleus accumbens (NAcc) plays a critical role in supporting drug self-administration (15, 16). Structurally, through its white-matter connections, NAcc projections then propagate signals through ascending prefrontal-striatal loops thought to convert affective impulses into motivated action (17–19). Functionally, NAcc activity in response to drug cues may predict relapse to stimulant use in human patients after leaving treatment (8). If NAcc activity can promote relapse in nonhuman as well as human models, then structural connections to the NAcc might modulate that activity. Specifically, both retrograde and anterograde tracer studies of nonhuman primates indicate that the NAcc receives glutamatergic projections from anterior aspects of the insula (18, 20, 21). The NAcc also receives glutamatergic projections from several amygdalar nuclei [including the basolateral, basal, basal accessory, central, and periamygdaloid nuclei (21–23)]. Finally, the striatum receives glutamatergic projections from prefrontal cortex (PFC) along a ventromedial to dorsolateral gradient. Specifically, ventromedial aspects of the striatum (including the NAcc) receive projections from orbitofrontal and ventromedial PFC regions, whereas dorsal regions of the striatum receive projections from more dorsolateral PFC regions (24, 25). While tracer studies do not describe the

Author affiliations: [a]Center for Cognitive and Decision Sciences, University of Basel, 4055 Basel, Switzerland; [b]Department of Psychology, Stanford University, Stanford, CA 94305-2130; [c]VA Palo Alto Health Care System, Palo Alto, CA 94304; and [d]Department of Psychological Science, University of Arkansas, Fayetteville, AR 72701

Author contributions: L.T., K.H.M., J.K.L., and B.K. designed research; L.T., K.H.M., and B.K. performed research; L.T., K.H.M., J.K.L., and B.K. analyzed data; L.T., K.H.M., C.B.P., J.K.L., and B.K. wrote the paper; and C.B.P. and B.K. did project administration.

The authors declare no competing interest.

This article is a PNAS Direct Submission.

[1]To whom correspondence may be addressed. Email: loreen.tisdall@unibas.ch.

This article contains supporting information online at http://www.pnas.org/lookup/suppl/doi:10.1073/pnas.2116703119/-/DCSupplemental.

Published June 21, 2022.

complete trajectory of these white matter tracts, they do confirm that the NAcc receives projections from anterior insula, amygdala, and medial PFC in nonhuman primates, which provides a strong anatomical foundation for inferring the existence of these connections in humans (18). We therefore sought to characterize the trajectory and structural characteristics of these prominent white matter tracts projecting to the NAcc in humans (or a "conNAcctome") (Fig. 1*A*) using diffusion-weighted magnetic resonance imaging (DMRI).

DMRI tractography offers a noninvasive method for tracking and characterizing brain structural connections (26, 27) that have previously been identified using more invasive methods [e.g., chemical tracing studies (28) or tissue clearing (29, 30)]. Different DMRI measures model the movement of water in the brain (or conversely, its occlusion) to support inference of underlying fiber bundles. For example, commonly used but distinct diffusion metrics include fractional anisotropy (FA), axial diffusivity (AD), radial diffusivity (RD), and mean diffusivity (MD) (27, 31). Reduction of brain lipids using multiple methods [e.g., lipid removal (32), myelin-deficient mice (33, 34), and other animal models (35)] can causally and predictably alter these diffusion metrics (e.g., decreasing FA while increasing RD), implying that they may partially index lipid coherence and/or myelination (34). Increased FA has commonly been associated with tract coherence, based on the implication that tracts with greater coherence might more effectively transmit neural signals. Decreased RD has further been linked to microstructural properties of brain tissue [e.g., fiber spread (36), cell and axon density (37), and axon myelination (33, 35, 38)].

Recent meta-analyses of DMRI studies of addiction suggest that patients with stimulant use disorder may have lower overall neural white matter coherence relative to healthy controls (31, 38). Most of this research, however, has employed whole brain approaches (such as tract-based spatial statistics [TBSS]), or focused on prominent large white-matter tracts [e.g., the corpus callosum and inferior longitudinal fasciculus (39–43)], rather than smaller tracts which project to subcortical regions (like the NAcc). Thus, the relevance of the structure of these conNAcctome tracts (Fig. 1*A*) for stimulant use, maintenance, and relapse has not yet been characterized.

DMRI studies of healthy individuals, however, have begun to suggest more precise links between structural properties of projections from cortical regions to the NAcc and individual differences in affect and cognition, and some of these may hold relevance for addiction. First, structural properties of a tract connecting the medial prefrontal cortex (MPFC) to the NAcc have been associated with impulsivity in adults [or valuing present over larger future rewards (44)], and early onset of binge drinking in adolescents (45). Second, we have found associations of measures of right anterior insula (AIns)-NAcc tract coherence with reduced risk seeking (46) and increased control of impulsive responses in the face of large incentives (47). These findings fit with extensive previous work implicating structural properties and correlated activity particularly in the right AIns-NAcc tract region (48) with inhibitory control (49). Third, structural properties of the amygdala (Amy)-NAcc tract have been associated with novelty seeking (50) and impulsivity (51). Fourth, we have reported associations of midbrain-NAcc tract coherence with impulsivity and stimulant use disorder diagnosis, but not with subsequent relapse (52). Addiction initiation and relapse, however, may recruit different psychological processes and associated neural circuits (14, 53, 54).

Here, we examined whether diffusion metrics of unidirectional white-matter projections to the NAcc from the MPFC, AIns [particularly on the right given previous findings (46, 47)], and Amy might predict relapse to stimulant use. We predicted that decreased diffusion metrics in these conNAcctome tracts might predict relapse to stimulant use (up to 6 mo after completing treatment) (46, 47). Since previous findings indicated that the structural coherence of a distinct tract connecting the midbrain to the NAcc was related to stimulant use diagnosis but not relapse, we used this midbrain-NAcc tract as a control comparison to test for double-dissociations (52).

Results

Sample characteristics. We examined the association of the structure of conNAcctome tracts with relapse to stimulant drug use in a sample of 60 SUD patients, comprising 30 individuals who had abstained and 30 individuals who had relapsed within

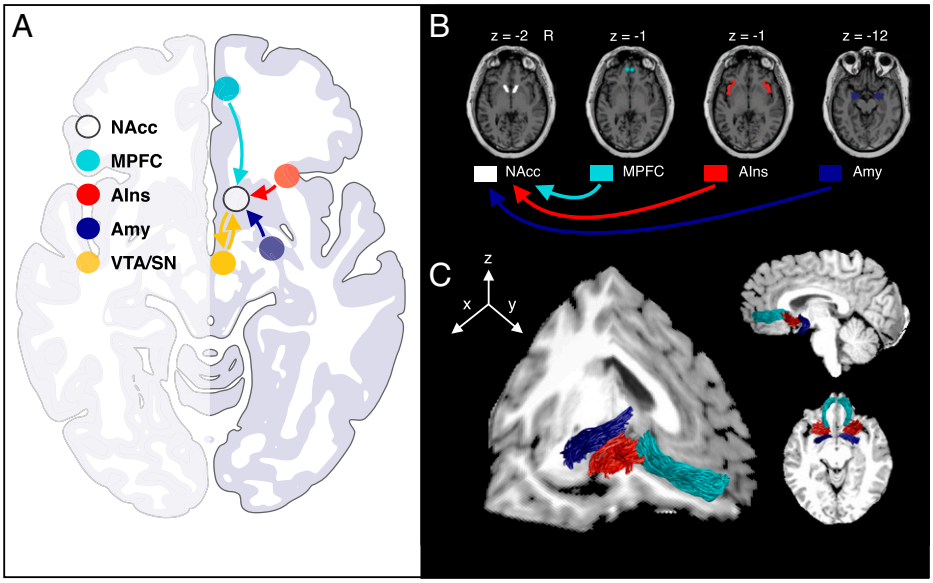

Fig. 1. Tracing conNAcctome tracts. (*A*) Schematic of predicted conNAcctome tracts (in MNI space; z = –10). (*B*) VOIs used for tractography. (*C*) ConNAcctome tract renderings. All VOIs and renderings shown for a representative individual in their native space. VTA/SN, dopaminergic midbrain regions including ventral tegmental area, substantia nigra, and parabrachial nucleus.

6 mo after release from treatment (10 additional patients were lost to follow-up prior to 6 mo and were therefore excluded from analysis; *SI Appendix*, Fig. S1 and Table S1). Consistent with previously reported relapse rates (7, 8), 15 SUD patients (25% of the patient sample) had relapsed after 2 mo (60 d). Thus, 50% of all patients who relapsed within the follow-up period had relapsed within the first 2 mo of release from treatment (*SI Appendix*, Fig. S2). Complete demographic information was obtained for all 60 SUD patients included in the current analyses. Four individuals (two relapsers and two abstainers) did not provide information about their years of use, and one (relapsed) individual did not complete the delay discounting questionnaire. As a result, the primary analyses involving structural data were performed on 60 patients, while control analyses involving demographic, clinical or personality variables were performed on 60, 56, and 55 patients, respectively.

Tract profiles and diffusion metrics. All tracts (i.e., MPFC-NAcc, AIns-NAcc, and Amy-NAcc) were successfully resolved in all participants (seed and target volumes of interest [VOIs] along with rendered tracts are shown in Fig. 1 *B* and *C*). Plotting participants' tract profiles together revealed similar patterns of diffusion metrics along the trajectory of each tract, as described in diffusion metric profiles documented in major white matter tracts (e.g., the corpus callosum and corticospinal tract) (55) (*SI Appendix*, Fig. S3). Based on this similarity across individuals, we computed and visualized average diffusion metrics for each of the three conNAcctome tracts of interest (*SI Appendix*, Fig. S3). Consistent with previous findings, both diffusion metric profiles and their associations with outcomes were expected to vary along each tract's trajectory (55).

Analyses focused on RD as the primary diffusion metric of interest, given its demonstrated links to tissue microstructure (33, 35, 37, 38), enhanced measurement properties relative to other diffusion metrics (56), and robust association with individual differences in impulsivity (52). RD may therefore offer a further close proxy for structural differences affecting signal transfer between brain regions. To facilitate comparison across different diffusion metrics (e.g., FA), we calculated inverse RD, such that higher values represent reduced perpendicular diffusivity (*SI Appendix*, *SI Methods*). To increase analytic sensitivity, the association of inverse RD with relapse status was evaluated along multiple nodes of each tract of interest, and corrections for multiple comparison were performed using permutation methods (55, 57) (*SI Appendix*, *SI Methods*).

Association of diffusion metrics with relapse. Inverse RD in the right AIns-NAcc tract was significantly associated with relapse status at the 6-mo follow-up assessment ($P < 0.05$, corrected; Fig. 2*C*; *SI Appendix*, Table S2). Specifically, higher inverse RD in a cluster of 33 consecutive nodes along the right AIns-NAcc tract predicted relapse (odds ratio [OR] = 0.39, z = –2.73, $P = 0.0063$), and this observed cluster exceeded the required extent of 28 nodes determined with permutation testing. Transforming individuals' tracts into a common MNI space revealed that the cluster extended from mean MNI coordinates 30, 15, −11 to 23, 13, −11, a distance of ∼6.3 mm. The same analytical approach (combining node-wise logistic regression

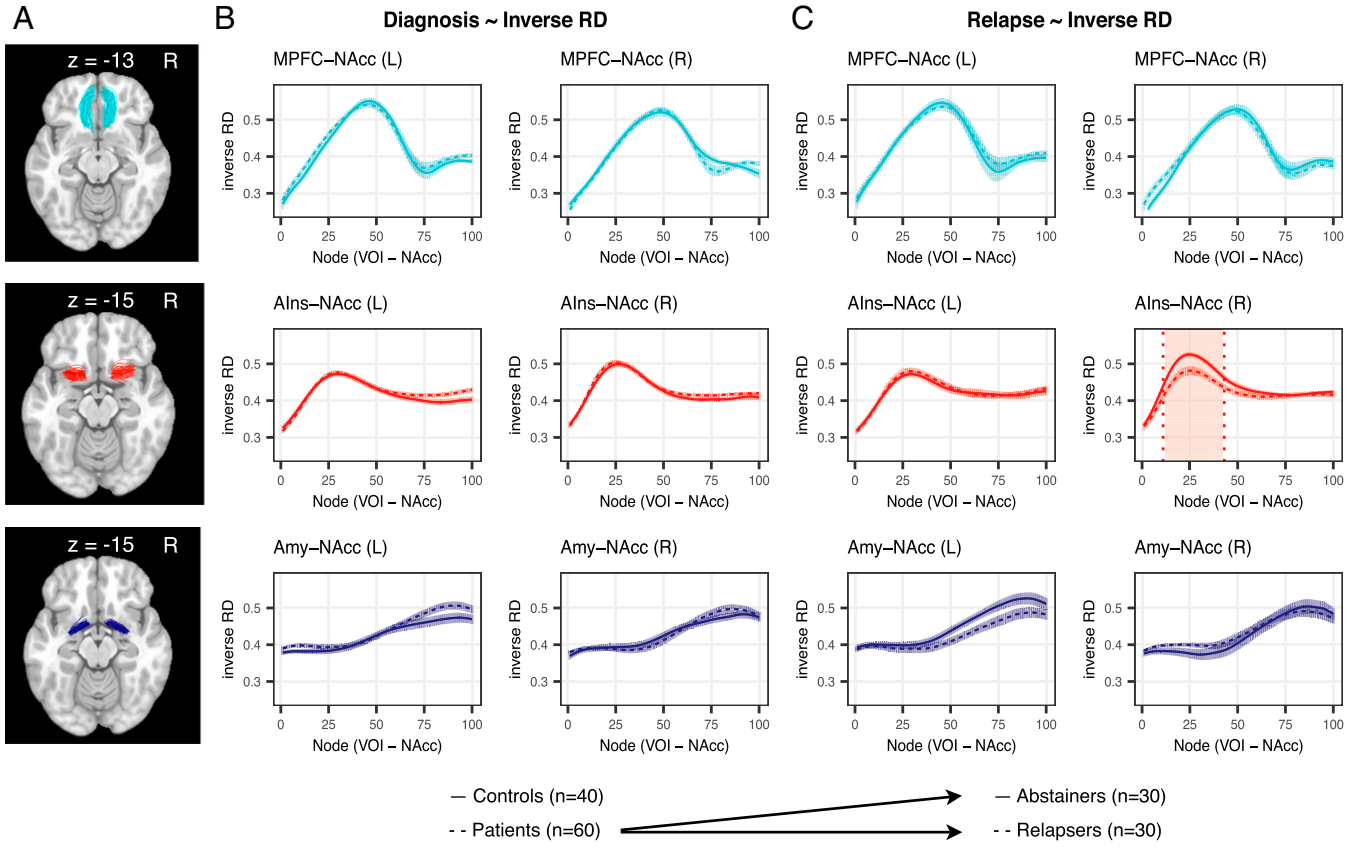

Fig. 2. Association of tract diffusion metrics with SUD diagnosis and relapse to stimulant use at 6-mo follow-up. (*A*) Group template of conNAcctome tracts (in MNI space). (*B*) Association of inverse RD in MPFC-NAcc (first row), AIns-NAcc (second row) and Amy-NAcc (third row) tracts with SUD diagnosis. (*C*) Association of inverse RD in MPFC-NAcc (first row), AIns-NAcc (second row) and Amy-NAcc (third row) tracts with relapse to stimulant use. Note that the x-axis represents the 100 equidistant nodes along the tract, the *y* axis represents the raw inverse RD metric (i.e., not standardized or controlling for confounds). Shaded areas represent SEM.

analyses with permutation testing) revealed that left AIns-NAcc and bilateral MPFC-NAcc inverse RD were not significantly associated with relapse, since the observed number of consecutive nodes significantly associated with relapse fell below the required number determined by permutation testing (observed/required number of nodes for left AIns-NAcc = 0/28; for left and right MPFC-NAcc = 0/23 and 0/25, respectively). An additional negative association of left Amy-NAcc tract inverse RD with relapse ($P < 0.05$, uncorrected; Fig. 2*C*, *Bottom* row) did not exceed the significance threshold (observed/required number of nodes = 20/36; $P > 0.05$, corrected). Further, the association of right Amy-NAcc tract inverse RD with relapse was not significant (observed/required number of nodes = 0/34). The significant association of right AIns-NAcc inverse RD with relapse remained robust even after exhaustively controlling for potential confounds in models that included demographic (including age and sex), clinical (including self-reported craving, negative mood, and years of use) (5), and methodological (head motion) variables (Fig. 3*A* and *SI Appendix*; see *SI Appendix*, Table S2 for model estimates and *SI Appendix*, Fig. S4 for bivariate correlations). Following previous work (52), the association between right AIns-NAcc inverse RD and relapse status also remained robust after controlling for individual differences in impulsivity (58, 59) (*SI Appendix*, Table S2). A similar association of right AIns-NAcc diffusion metrics with relapse status was also apparent after substituting inverse RD with the more commonly used FA metric (observed/required number of nodes = 25/25; *SI Appendix*, Tables S3 and Figs. S5 and S6).

In contrast to relapse, inverse RD of the three tracts of interest was not associated with diagnosis (Fig. 2*B*). Based on a sample of 40 healthy controls and 60 SUD patients (*SI Appendix*, Table S4), node-wise logistic regression analyses revealed no significant associations ($P > 0.05$, uncorrected) between inverse RD and SUD diagnosis at any node for the left or right MPFC-NAcc tracts, left or right Amy-NAcc tracts, or the right AIns-NAcc tract. An association at two consecutive nodes of the left AIns-NAcc tract ($P < 0.05$, uncorrected) did not exceed the significance threshold ($P > 0.05$ corrected).

The contribution of tract structural metrics to the classification of relapse versus that of demographic, clinical, personality, and

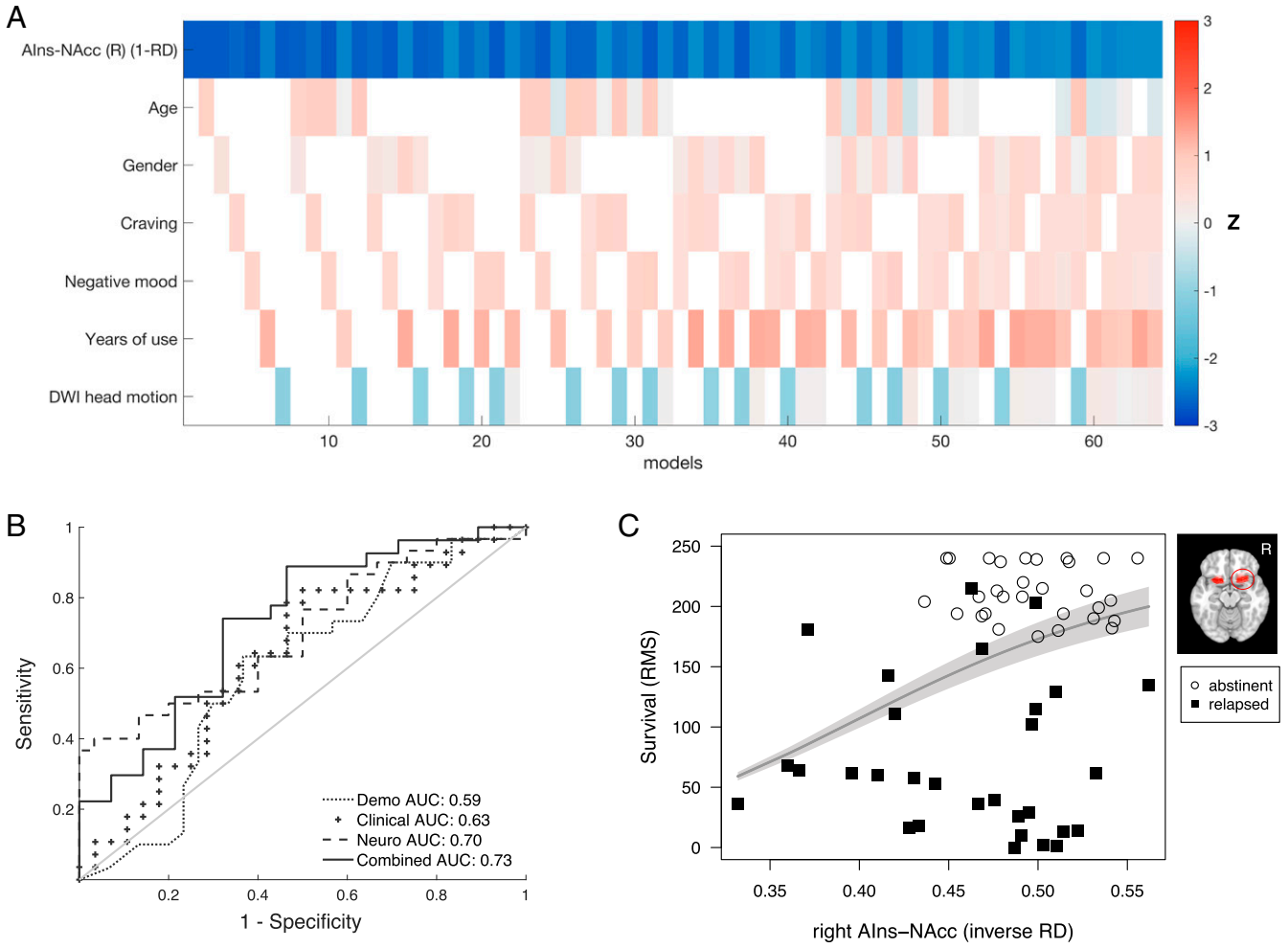

Fig. 3. Predicting relapse with right AIns-NAcc tract diffusion metrics. (*A*) A "Regression Multiverse" analysis verifies the robustness of the association between inverse RD and relapse. Rows represent individual predictor variables; columns represent exhaustive combinatorial specifications of relapse models; colors represent the effect size of a variable (row), given the specific grouping of predictor variables in the model (column). All models tested contained right AIns-NAcc inverse RD but varied with respect to the inclusion of other demographic, clinical, and methodological variables. Statistics for a subset of models are presented in *SI Appendix*, Table S2. (*B*) Receiver operating characteristic (ROC) curves for the classification of relapse status (i.e., yes versus no) at 6 mo after treatment release from neural (right AIns-NAcc inverse RD), demographic (age and sex), clinical (years of use, negative mood, craving), methodological (head motion), and personality (BIS, delay discounting factor k) predictor variables. Curves represent the sensitivity and specificity of separate neural, demographic, clinical, and combined (neural, demographic, clinical, methodological, personality) relapse models. The gray diagonal line represents chance (i.e., 50/50) classification of relapse status at six months following release from treatment. (*C*) Model-based (i.e., predicted) mean survival time as a function of right AIns-NAcc tract inverse RD [computation based on observed time to relapse (days)]. Gray line presents the restricted mean survival time, shaded gray area represents the parameterized SE. Black squares are observed days to relapse for relapsers, white circles are follow-up times for abstainers.

methodological variables was further compared by calculating area under the curve (AUC) estimates for receiver operating characteristic (ROC) curves (Fig. 3*B*) (*SI Appendix*, Table S2). The AUC values of different relapse models suggested that relapse classification using only a neural marker performed better than a model of relapse containing demographic or clinical variables and was only marginally superseded by a combined model. Explained variance (pseudo-R^2) estimates further suggested that the model containing only the right AIns-NAcc structural marker explained more variance (22%) than either demographic (2%), or clinical (6%) models, with most variance being explained by a combined model (26%). Due to the increased number of variables in the combined model (relative to our sample size), however, this increase in explained variance was offset by a higher Akaike information criterion AIC and lower estimates for leave-one-out cross-validation estimates of prediction accuracy (*SI Appendix*, Table S2). The amount of variance explained by the structural model was similar to estimates reported in previous studies using brain data to predict substance use diagnosis and relapse (8, 52). Moreover, the relatively lower variance accounted for by demographic and clinical variables also aligned with previously reported estimates (60–62).

Survival analysis using a Cox-proportional hazards model further confirmed that the association between right AIns-NAcc inverse RD and relapse was not limited to a binary definition of relapse but additionally extended to a continuous definition in terms of days until relapse. After controlling for age, sex, and head motion, lower right AIns-NAcc inverse RD was associated with risk of sooner relapse (HR = 0.62; 95% confidence interval [CI] = 0.44–0.87; $P = 0.005$). The concordance rate for this model was 0.644 (SE = 0.045), implying that for 64.4% of pairs of SUD patients, the individual with the lower right AIns-NAcc inverse RD relapsed sooner. For transparent visualization of this association between right AIns-NAcc inverse RD and time to relapse, we plotted the individually observed time to relapse along with the predicted restricted mean survival time (Fig. 3*C*). Similar patterns were observed for classification and survival analyses using right AIns-NAcc FA (*SI Appendix*, Fig. S6).

Double dissociation of SUD diagnosis and relapse. Previous work based on a subset of participants in the current study (52) reported a negative association of FA in a tract connecting the dopaminergic midbrain (including the VTA) with the NAcc and SUD diagnosis, but not with relapse (52). In contrast, the current analyses revealed an association of right AIns-NAcc tract inverse RD with relapse to stimulant use, but not with SUD diagnosis (Fig. 2). To directly compare the previous and current results by testing for a double dissociation, we extended the previous sample to include all of the individuals in the current analyses, and then reanalyzed the VTA-NAcc tract data with the improved analytical pipeline developed for the current study (see *SI Appendix* for further details). The reanalysis of VTA-NAcc tract metrics based on a larger sample and optimized analyses produced similar findings to those reported previously (52). Specifically, FA in an extended bilateral cluster of VTA-NAcc tract nodes was associated with SUD diagnosis ($P < 0.05$, corrected), but not relapse status six months after treatment. Combined with the currently reported association of right AIns-NAcc inverse RD and relapse, these findings indicate a double dissociation of neural structural markers associated with SUD diagnosis versus relapse to stimulant drug use (Fig. 4).

To visualize this structural double dissociation, for each tract we plotted the summary indices extracted from the cluster of nodes that demonstrated a significant association with the predicted outcome (i.e., nodes 1–95 for VTA-NAcc association with diagnosis and nodes 11–43 for right AIns-NAcc association with relapse) against both SUD diagnosis (Fig. 4*B*) and relapse (Fig. 4*C*). To maintain consistency with previous findings, we depicted the double dissociation using FA for the VTA-NAcc tract (52), but inverse RD for the AIns-NAcc tract. Importantly, inverse RD and FA for the right AIns-NAcc were highly correlated ($r_S = 0.82$, *SI Appendix*, Fig. S4), possibly explaining their similar associations with relapse (*SI Appendix*, Fig. S5). The double dissociation held, however, when including FA for both tracts (*SI Appendix*, Fig. S7). Together, these findings highlight the possibility that structural characteristics of different neural circuits converging on the same region (i.e., NAcc) may confer risk for different stages of addiction.

Discussion

By targeting tracts converging on the NAcc with a combination of diffusion-weighted neuroimaging and probabilistic tractography, we found that structural properties of white-matter tracts connecting the anterior insula (AIns) to the NAcc selectively predict relapse to stimulant use. Specifically, inverse RD of the right AIns-NAcc tract predicted relapse status up to 6 mo after treatment. This neural structural predictor outperformed alternative demographic, clinical, personality, and methodological predictors of relapse, and was further associated with time to relapse. Indeed, adoption of a "regression multiverse" analytic approach (63) supported the robustness of the estimated association of inverse RD with relapse against numerous potential confounds. Further, comparison with previous findings implicated a double dissociation of the association of the structure of different conNAcctome tracts with stimulant use disorder diagnosis versus relapse. Specifically, whereas reduced FA in the VTA-NAcc tract was associated with diagnosis but not relapse, reduced inverse RD (as well as FA) in the right AIns-NAcc tract was instead associated with relapse but not diagnosis (52). Contrary to predictions, however, structural qualities of other tracts connecting to the NAcc (i.e., MPFC-NAcc and Amy-NAcc tracts) were not significantly associated with SUD diagnosis or relapse.

These findings make several contributions to our current understanding of addiction and relapse. A first contribution involves localizing the prediction of relapse to specific cortical structural projections to the NAcc, which strengthens the case for brain-based models of addiction (13), and highlights the added value conferred by leveraging neuroimaging methods. A second contribution involves the specific association of relapse with structural qualities of the right AIns-NAcc tract but not MPFC-NAcc or Amy-NAcc tracts, possibly implicating functions related to cue-induced negative arousal rather than value integration or behavioral control (10, 14). Anterior insula activity has previously been implicated in relapse based on correlations with arousal and craving (14), which may be associated with a modulatory influence of AIns structural projections on NAcc activity (47). Specifically, we have proposed that AIns-NAcc tract coherence may blunt NAcc activity during motivated behavior, as in the case of "incentivized inhibition" (47). In the context of relapse, lower coherence (33, 35) of the AIns-NAcc tract might reduce inhibition of drug seeking after cue exposure, which could ultimately thwart intentions to remain abstinent. While human lesion studies have implicated the insula in smoking cessation (64), the localization of these effects to the anterior insula versus middle or posterior insula or adjacent striatum is presently unclear (65). The lateral specificity of

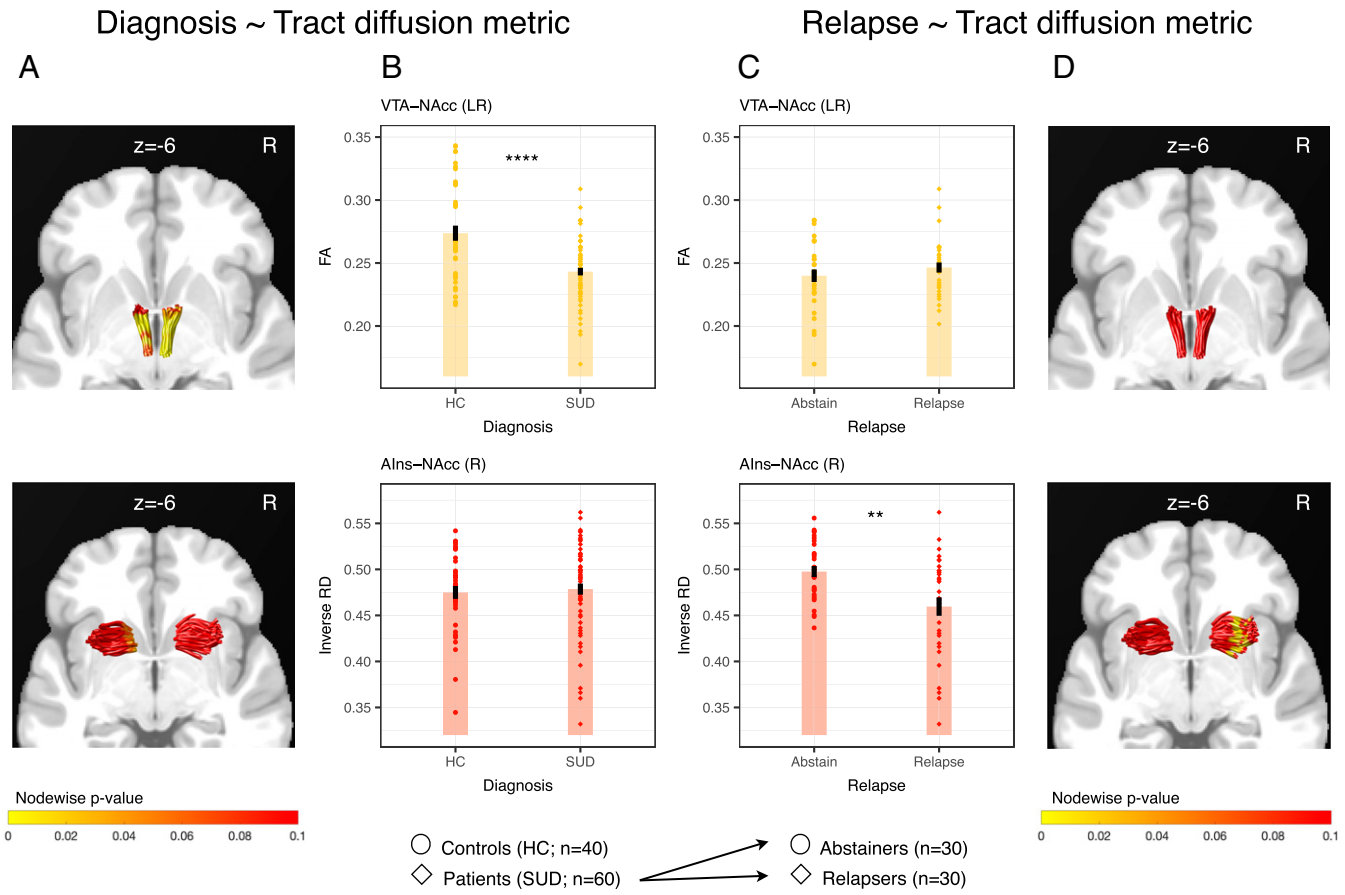

Fig. 4. Double dissociation of SUD diagnosis and relapse with VTA-NAcc (*Top*) and AIns-NAcc (*Bottom*) tract diffusion metrics. (*A*) Group tracts in MNI space with superimposed node-wise associations between tract diffusion metrics and SUD diagnosis. Each tube depicts the core trajectory of one individual's tract, transformed into MNI space. Colors indicate the node-wise *P* value for the association between tract diffusion metrics and SUD diagnosis. (*B*) SUD diagnosis as a function of tract metric. (*C*) Relapse to stimulant drug use as a function of tract metric. For (*B*) and (*C*), each colored point represents an individual, bars represent group means, black lines represent SEMs. Colored data points represent individuals' summary tract diffusion metrics for relapse-relevant node clusters of bilateral VTA-NAcc (nodes 1–95, FA) and right AIns-NAcc tracts (nodes 11–43, inverse RD). (*D*) Group tracts in MNI space with superimposed node-wise associations between tract diffusion metrics and relapse. Each tube represents the core trajectory of one individual's fiber tract, transformed into MNI space. Colors indicate the node-wise *P* value for the association between tract diffusion metrics and relapse to stimulant drug use. $^{**}P = 0.0026$; $^{****}P = 0.000053$.

this association to the right AIns-NAcc tract is consistent with previous research on risk taking (46, 47) and inhibitory control (47, 49). Importantly, although both the right AIns and adjacent right inferior frontal cortex are consistently activated by demands for inhibitory control, these regions may serve dissociable functional roles (49). Specifically, activity in the right AIns seems to respond preferentially to the early detection of salient events, whereas activity in the right inferior frontal cortex seems to respond preferentially to demands for inhibiting ongoing motor activity. Further, white-matter abnormalities near the right AIns have been reported in both stimulant-dependent individuals and their unaffected siblings relative to healthy controls (54). Reduced coherence in this region has additionally been associated with poorer behavioral implementation of inhibitory control. These convergent findings not only suggest a rightward locus of inhibitory control near the anterior insula, but further suggest a neural marker of heritable risk for stimulant drug use (rather than a consequence of chronic use) (54).

A third contribution involves discovery of a double dissociation of the association of distinct conNAcctome tract structural qualities (i.e., VTA-NAcc vs. right AIns-NAcc tract) with stimulant use disorder diagnosis versus relapse. This distinction might imply that different neural structural and functional connections are related to the onset versus maintenance of disordered stimulant use. By revealing the right AIns-NAcc tract as a structural target for predicting relapse, these results imply that, unlike stimulant use disorder diagnosis (52), cortical rather than subcortical projections to the NAcc may play a more prominent role in preventing relapse to stimulant drug use. Functionally, these structural findings align with proposals that impulsivity and compulsivity may drive different sequential stages of the addiction cycle (53). While impulsivity may contribute to an individual's path into excessive drug consumption and eventual dependence, compulsivity may instead contribute to drug use maintenance and trigger relapse after leaving treatment. Our previous findings (52) confirm the first component by demonstrating an association of decreased inferior VTA-NAcc tract coherence with individual differences in impulsivity, as well as SUD diagnosis. In turn, the previously documented association of right AIns-NAcc tract coherence with incentivized inhibition performance (46, 47) might reveal aspects of a second component of compulsivity. Theorists have proposed that the shift from impulsivity fueling early stages of addiction to compulsivity fueling later stages of addiction (including relapse) co-occurs with a shift from positive reinforcement mechanisms to negative reinforcement and automaticity mechanisms driving drug seeking behavior (14, 66, 67). If reduced right AIns-NAcc structural organization diminishes input associated with negative arousal, liberating NAcc activity

associated with positive arousal and approach, over time such a dynamic might facilitate compulsive behavior. Since the design of the current research did not include a reliable and valid measure of individual differences in compulsivity, future research will need to directly test whether measures of compulsivity might help account for the association between right AIns-NAcc tract diffusion metrics and relapse to stimulant drug use.

This research features several strengths. First, the work combined probabilistic tractography with predicted volumes of interest, which supported the identification, visualization, and measurement of small white-matter tracts that might elude whole brain analyses. Second, the hypotheses and main analyses were inspired by comparative research that confirms known structural connections and were preregistered, limiting researcher degrees of freedom. Third, the longitudinal research design incorporated temporal precedence, facilitating discovery of a double dissociation of structural markers for stimulant use disorder diagnosis versus relapse in the same individuals. Fourth, tests of neural predictors were optimized for multiple hypothesis testing by computing permutation-based cluster extents to infer statistical significance (55, 57). Fifth, although noninvasive neuroimaging measures necessarily limit inferences about underlying structural physiology, the primary diffusion metric utilized (i.e., inverse RD) can index properties of cell membranes and myelination, and has shown the most robust associations with individual differences in previous research (33, 35, 38, 52). Importantly, supplementary analyses indicate that these diffusion metrics also feature favorable measurement qualities for assessing individual differences (i.e., high test–retest reliability) (*SI Appendix*, Fig. S8) and are not attributable to local variation in signal to noise ratio or tissue volume (47, 68). Given these methodological strengths, the present findings imply specific associations between local variation in brain tract structure and individual differences related to addiction.

This research also has some limitations. First, the research plan did not explicitly include measures of functional activity. Auxiliary analyses of an associated functional study did, however, imply that correlated activity between the right AIns and NAcc during viewing of drug cues (but not otherwise) was associated with subsequent abstinence (*SI Appendix*, Fig. S9 (8)). Second, although abstinent versus relapsed SUD patients were comparable with respect to demographic and clinical variables (and controlling for these did not alter observed associations between inverse RD and relapse), unmeasured clinical variables might still influence comparisons. The existing literature on factors associated with relapse to drug use (5) has not, however, identified obvious alternative confounding variables. Further, regression multiverse analyses suggested that the association of inverse RD with relapse remained robust against control for combinations of multiple potential confounds (Fig. 3*A*). Third and finally, as in all clinical research, the observed associations may not generalize beyond the sample and disorder under study. For instance, neural correlates of substance use onset and relapse may vary across different drug classes [e.g., opioids, alcohol, nicotine (43)], motivating further exploration in both animal models (69) and human patients (5, 14, 39, 53). Reassuringly, however, cross-validation analyses suggested that the currently observed associations of tract diffusion metrics with relapse appeared at least to generalize across individuals in the sample (*SI Appendix*, Tables S2 and S3).

The discovery of a structural marker for relapse raises several possibilities for future exploration. Physiologically, new tools (e.g., optogenetics, viral tracing, and tissue clearing) could bridge to animal models of relapse and further elucidate how changes in myelination influence targeted tracts (such as the AIns-NAcc tract), and modulate stimulant drug use onset and relapse (69, 70). Conceptually, identification and quantification of conNAcctome tract qualities in humans may inspire more precise characterization of circuits implicated in clinical disorders of impulse control, potentially informing the interpretation and prediction of functional deficits and intervention targets. Clinically, in contrast to extensive distributed networks (71) or projections lacking demonstrated functional relevance to addiction (38, 43), precise qualities of AIns-NAcc tract structure may predict vulnerability to relapse. Such knowledge may eventually not only guide decisions about who can benefit most from interventions, but also identify new targets for intervention with therapy, pharmacology, or even targeted stimulation (72).

Materials and Methods

The study was approved by the institutional review boards of the Stanford University School of Medicine and Research and Development Office of the Veterans Affairs Palo Alto Health Care System. Prior to participating in the study, all individuals gave written informed consent. The study's design and hypotheses were preregistered (https://aspredicted.org/9rf2e.pdf).

Participants. An overview of the study sample and composition is presented in the form of a consort plot (*SI Appendix*, Fig. S1).

Patients. We recruited 78 detoxified patients with SUD from two residential SUD treatment programs: at the Veterans Affairs Palo Alto Health Care System, Palo Alto, California (see also ref. 8), and at the Epiphany Center, San Francisco, California (a holistic residential recovery program for women). Clinicians and/or a member of the research team completed a full history and clinical interview with every patient, comprising diagnostic questions about past and current psychiatric symptoms and/or SUD based on DSM-5 criteria. Interested individuals were screened and excluded from participation if they took medications capable of influencing vasoreactivity (e.g., cardiac medications, ibuprofen) or central dopaminergic activity (e.g., stimulants, antipsychotics), had a history of traumatic head injury, had a history of serious mental illness (e.g., mania, psychosis), or had compromised safety for magnetic resonance scanning (e.g., ferromagnetic material in the head or body). We then recruited eligible patients with a current diagnosis of SUD (e.g., methamphetamine, crack and powder cocaine). Abstinence throughout treatment and before each scan was verified via urine toxicology tests. The eligibility screening tool confirmed that the primary reason for seeking treatment involved problematic stimulant use. Eight patients were excluded prior to analysis due to excessive head motion, resulting in a sample of 70 SUD patients for analysis.

With respect to treatment outcome at six months, we obtained a comparable sample of individuals who had abstained from stimulant use ($n = 30$, 24 [80%] males, 39.5 $\pm$ 12.5 y old) and who had relapsed to stimulant use ($n = 30$, 26 [86.7%] males, 42.3 $\pm$ 10.9 y old; *SI Appendix*, Table S1). Ten SUD patients (7 [70%] males, 44.1 $\pm$ 12.2 y old) were lost to follow-up. Regardless of outcome and availability at follow-up, SUD patients who abstained versus relapsed were comparable with respect to methodological (e.g., head motion), demographic (e.g., age, sex, education), and clinical (e.g., anxiety, depression, and primary stimulants used) variables (*SI Appendix*, Table S1).

Healthy controls. Forty-four healthy control participants were recruited from the Stanford University Paid Psychology Experimental pool and the San Francisco Bay Area community. Exclusion criteria were the same as for SUD patients, with the added exclusion of any current or prior history of alcohol or substance use disorder. We did not ascertain detailed information about healthy control participants' recreational substance use, but instead used diagnostic criteria to exclude for lifetime alcohol and substance use disorders (73). Data from four participants were excluded prior to analysis due to excessive head motion during scanning, leaving 40 healthy controls (57% male, 32.7 $\pm$ 11.8 y old) for analyses. SUD patients and healthy controls varied on several demographic and clinical variables (*SI Appendix*, Table S4), but had comparable head motion during scanning (see also ref. 52).

Study protocol. Participants first provided informed consent and were then scanned using magnetic resonance imaging (MRI) to acquire anatomical and diffusion-weighted images. The neuroimaging scans were acquired while

participants were enrolled in the residential treatment program, with a period approximately 2 wk into treatment targeted for scanning. We also collected functional scans, but since these are not critical for the current analyses, they are not described further [except in the *SI Appendix, SI Methods* and Fig. S9; see (8)]. After scanning, participants completed a battery of self-report questionnaires, including the Ten Item Personality Inventory (74), the Barratt Impulsivity Scale-11 (58), a 21-item Kirby Monetary Choice Questionnaire (59), the Behavioral Inhibition Scale/Behavioral Activation Scale (75), and Beck Depression Inventory (76). For SUD patients, stimulant use was assessed via phone interview approximately 1, 3, and 6 mo after discharge from treatment using the Time-Line Follow-Back method (77), which has been shown to have moderate-to-high consistency with urine toxicology screens (78). As part of the follow-up interviews, patients completed the Brief Addiction Monitor (79), which facilitated assessment of clinical and affective variables which may contribute to relapse, including craving and negative mood (5). The dependent variable of relapse was defined as reporting any stimulant use in the time since treatment discharge or the previous assessment. Participants in the healthy control group did not complete any follow-up assessments.

All participants (both patients and controls) received a base payment of $100 in the form of an Amazon.com gift card and could earn an additional $0–$30 based on their performance in other tasks that occurred during the scanning session. Patients were additionally compensated $50 (also in the form of an Amazon.com gift card) for each completed follow-up interview.

Neuroimaging data acquisition and analysis. Structural and diffusion-weighted imaging sequences were acquired and processed as described in previous tractography studies (46, 47, 52) (*SI Appendix, SI Methods*).

Verifying robustness and ruling out confounds. Given the (right) lateral specificity of the key structural predictor, we performed supplementary robustness checks, including examination of hemispheric differences in voxel-wise signal-to-noise ratio (SNR) in the diffusion-weighted signal, as well as the white matter volume of reconstructed left and right AIns-NAcc tracts. These analyses indicated that neither SNR nor tract volume could account for the observed ability of right but not left AIns-NAcc tract diffusion metrics to predict relapse to stimulant use (*SI Appendix, SI Methods*). To further verify the robustness of the findings, we computed test-retest reliability for the reported conNAcctome tract diffusion metrics in an independent sample ($n = 9$). Regardless of tract metric, these analyses revealed high test–retest reliability for the right AIns-NAcc tract (all intraclass correlation coefficients >0.9) (*SI Appendix, SI Methods* and Fig. S8).

Because previous research reported alterations in gray matter volume and functional connectivity associated with substance use disorder (80, 81), we further tested whether these measures were related to relapse in the current cohort. Gray matter volume was not related to relapse in any of the conNAcctome VOIs (*SI Appendix, SI Methods*). For abstainers (but not relapsers or healthy controls), correlated activity between right AIns and NAcc increased during exposure to drug cues (consistent with the notion that AIns-NAcc communication promotes abstinence), but not otherwise (*SI Appendix, SI Methods* and Fig. S9) (8). This association, however, could not statistically account for the association of right AIns-NAcc tract diffusion metrics with relapse.

Data Availability. Anonymized behavioral and tractography indices data have been deposited in Open Science Framework (https://osf.io/z35yn/). Previously published data were used for this work. A subset of our findings reports a double dissociation between the structure of different brain tracts and relapse to stimulant drug use versus previous diagnosis of SUD (Fig. 4). For these analyses, we replicate and extend the findings reported previously by MacNiven et al. (52), by applying analytical methods to a larger data set. Furthermore, we present statistical analyses and provide visualizations for the double dissociation. The original findings are referenced throughout the manuscript.

ACKNOWLEDGMENTS. We thank Emily L.S. Jensen and Sarah I. Hudson for their help with data acquisition, as well as spanlab and three anonymous reviewers for comments on previous drafts. This research was supported by a NeuroChoice Initiative "Big Ideas" grant from Stanford's Wu Tsai Neurosciences Institute and the National Institute of Health (5P50DA042012-05 to B.K.). L.T. was funded through an Early PostDoc.Mobility Fellowship (Grant P2BSP1_188172) from the Swiss National Science Foundation.

1. United Nations Office on Drugs and Crime, World Drug Report 2020. https://wdr.unodc.org/wdr2020/en/index2020.html. Accessed 9 June 2022.
2. M. Ezzati, A. D. Lopez, A. Rodgers, C. J. L. Murray, *Comparative Quantification of Health Risks: Global and Regional Burden of Disease Attributable to Selected Major Risk Factors* (World Health Organization, 2004).
3. M. L. Dennis, M. A. Foss, C. K. Scott, An eight-year perspective on the relationship between the duration of abstinence and other aspects of recovery. *Eval. Rev.* **31**, 585–612 (2007).
4. B. J. Everitt, A. Dickinson, T. W. Robbins, The neuropsychological basis of addictive behaviour. *Brain Res. Brain Res. Rev.* **36**, 129–138 (2001).
5. M. Reske, M. P. Paulus, Predicting treatment outcome in stimulant dependence. *Ann. N. Y. Acad. Sci.* **1141**, 270–283 (2008).
6. L. J. Wang *et al.*, Difference in long-term relapse rates between youths with ketamine use and those with stimulants use. *Subst. Abuse Treat. Prev. Policy* **13**, 50 (2018).
7. M. L. Brecht, D. Herbeck, Time to relapse following treatment for methamphetamine use: A long-term perspective on patterns and predictors. *Drug Alcohol Depend.* **139**, 18–25 (2014).
8. K. H. MacNiven *et al.*, Association of neural responses to drug cues with subsequent relapse to stimulant use. *JAMA Netw. Open* **1**, e186466–e186466 (2018).
9. B. Adinoff *et al.*, Decision-making processes as predictors of relapse and subsequent use in stimulant-dependent patients. *Am. J. Drug Alcohol Abuse* **42**, 88–97 (2016).
10. K. D. Ersche, G. B. Williams, T. W. Robbins, E. T. Bullmore, Meta-analysis of structural brain abnormalities associated with stimulant drug dependence and neuroimaging of addiction vulnerability and resilience. *Curr. Opin. Neurobiol.* **23**, 615–624 (2013).
11. R. A. Rawson, R. Gonzales, P. Brethen, Treatment of methamphetamine use disorders: An update. *J. Subst. Abuse Treat.* **23**, 145–150 (2002).
12. B. Knutson, A. Heinz, Probing psychiatric symptoms with the monetary incentive delay task. *Biol. Psychiatry* **77**, 418–420 (2015).
13. N. D. Volkow, G. Koob, Brain disease model of addiction: Why is it so controversial? *Lancet Psychiatry* **2**, 677–679 (2015).
14. G. F. Koob, N. D. Volkow, Neurocircuitry of addiction. *Neuropsychopharmacology* **35**, 217–238 (2010).
15. R. A. Wise, M. A. Bozarth, Brain substrates for reinforcement and drug self-administration. *Prog. Neuropsychopharmacol.* **5**, 467–474 (1981).
16. G. Di Chiara, A. Imperato, Drugs abused by humans preferentially increase synaptic dopamine concentrations in the mesolimbic system of freely moving rats. *Proc. Natl. Acad. Sci. U.S.A.* **85**, 5274–5278 (1988).
17. G. J. Mogenson, D. L. Jones, C. Y. Yim, From motivation to action: Functional interface between the limbic system and the motor system. *Prog. Neurobiol.* **14**, 69–97 (1980).
18. S. N. Haber, B. Knutson, The reward circuit: Linking primate anatomy and human imaging. *Neuropsychopharmacology* **35**, 4–26 (2010).
19. G. R. Samanez-Larkin, B. Knutson, Decision making in the ageing brain: Changes in affective and motivational circuits. *Nat. Rev. Neurosci.* **16**, 278–289 (2015).
20. M. Chikama, N. R. McFarland, D. G. Amaral, S. N. Haber, Insular cortical projections to functional regions of the striatum correlate with cortical cytoarchitectonic organization in the primate. *J. Neurosci.* **17**, 9686–9705 (1997).
21. A. C. McHale, Y. T. Cho, J. L. Fudge, Cortical granularity shapes the organization of afferent paths to the amygdala and its striatal targets in nonhuman primate. *J. Neurosci.* **42**, 1436–1453 (2022).
22. F. T. Russchen, I. Bakst, D. G. Amaral, J. L. Price, The amygdalostriatal projections in the monkey. An anterograde tracing study. *Brain Res.* **329**, 241–257 (1985).
23. J. L. Fudge, K. Kunishio, P. Walsh, C. Richard, S. N. Haber, Amygdaloid projections to ventromedial striatal subterritories in the primate. *Neuroscience* **110**, 257–275 (2002).
24. E. Lynd-Balta, S. N. Haber, The organization of midbrain projections to the striatum in the primate: Sensorimotor-related striatum versus ventral striatum. *Neuroscience* **59**, 625–640 (1994).
25. S. N. Haber, Corticostriatal circuitry. *Dialogues Clin. Neurosci.* **18**, 7–21 (2016).
26. D. C. Alexander, T. B. Dyrby, M. Nilsson, H. Zhang, Imaging brain microstructure with diffusion MRI: Practicality and applications. *NMR Biomed.* **32**, e3841 (2019).
27. A. Lazari, I. Lipp, Can MRI measure myelin? Systematic review, qualitative assessment, and meta-analysis of studies validating microstructural imaging with myelin histology. *Neuroimage* **230**, 117744 (2021).
28. S. Jbabdi, J. F. Lehman, S. N. Haber, T. E. Behrens, Human and monkey ventral prefrontal fibers use the same organizational principles to reach their targets: Tracing versus tractography. *J. Neurosci.* **33**, 3190–3201 (2013).
29. K. Chung, K. Deisseroth, CLARITY for mapping the nervous system. *Nat. Methods* **10**, 508–513 (2013).
30. C. Leuze *et al.*, Comparison of diffusion MRI and CLARITY fiber orientation estimates in both gray and white matter regions of human and primate brain. *Neuroimage* **228**, 117692 (2021).
31. R. Suchting *et al.*, A meta-analysis of tract-based spatial statistics studies examining white matter integrity in cocaine use disorder. *Addict. Biol.* **26**, e12902 (2021).
32. C. Leuze *et al.*, The separate effects of lipids and proteins on brain MRI contrast revealed through tissue clearing. *Neuroimage* **156**, 412–422 (2017).
33. S. K. Song *et al.*, Dysmyelination revealed through MRI as increased radial (but unchanged axial) diffusion of water. *Neuroimage* **17**, 1429–1436 (2002).
34. X. Ou, S. W. Sun, H. F. Liang, S. K. Song, D. F. Gochberg, The MT pool size ratio and the DTI radial diffusivity may reflect the myelination in shiverer and control mice. *NMR Biomed.* **22**, 480–487 (2009).
35. V. A. Janve *et al.*, The radial diffusivity and magnetization transfer pool size ratio are sensitive markers for demyelination in a rat model of type III multiple sclerosis (MS) lesions. *Neuroimage* **74**, 298–305 (2013).
36. A. S. Choe, I. Stepniewska, D. C. Colvin, Z. Ding, A. W. Anderson, Validation of diffusion tensor MRI in the central nervous system using light microscopy: Quantitative comparison of fiber properties. *NMR Biomed.* **25**, 900–908 (2012).
37. H. B. Stolp *et al.*, Voxel-wise comparisons of cellular microstructure and diffusion-MRI in mouse hippocampus using 3D Bridging of Optically-clear histology with Neuroimaging Data (3D-BOND). *Sci. Rep.* **8**, 4011 (2018).
38. C. L. Beard *et al.*, Regional differences in white matter integrity in stimulant use disorders: A meta-analysis of diffusion tensor imaging studies. *Drug Alcohol Depend.* **201**, 29–37 (2019).

39. W. H. Hampton, I. M. Hanik, I. R. Olson, Substance abuse and white matter: Findings, limitations, and future of diffusion tensor imaging research. *Drug Alcohol Depend.* **197**, 288–298 (2019).
40. K. O. Lim *et al.*, Brain macrostructural and microstructural abnormalities in cocaine dependence. *Drug Alcohol Depend.* **92**, 164–172 (2008).
41. L. Ma *et al.*, A preliminary longitudinal study of white matter alteration in cocaine use disorder subjects. *Drug Alcohol Depend.* **173**, 39–46 (2017).
42. J. Xu *et al.*, White matter integrity is associated with treatment outcome measures in cocaine dependence. *Neuropsychopharmacology* **35**, 1541–1549 (2010).
43. J. Ottino-González *et al.*, White matter microstructure differences in individuals with dependence on cocaine, methamphetamine, and nicotine: Findings from the ENIGMA-Addiction working group. *Drug Alcohol Depend.* **230**, 109185 (2022).
44. W. H. Hampton, K. H. Alm, V. Venkatraman, T. Nugiel, I. R. Olson, Dissociable frontostriatal white matter connectivity underlies reward and motor impulsivity. *Neuroimage* **150**, 336–343 (2017).
45. A. M. Morales, S. A. Jones, G. Harman, J. Patching-Bunch, B. J. Nagel, Associations between nucleus accumbens structural connectivity, brain function, and initiation of binge drinking. *Addict. Biol.* **25**, e12767 (2020).
46. J. K. Leong, F. Pestilli, C. C. Wu, G. R. Samanez-Larkin, B. Knutson, White-matter tract connecting anterior insula to nucleus accumbens correlates with reduced preference for positively skewed gambles. *Neuron* **89**, 63–69 (2016).
47. J. K. Leong, K. H. MacNiven, G. R. Samanez-Larkin, B. Knutson, Distinct neural circuits support incentivized inhibition. *Neuroimage* **178**, 435–444 (2018).
48. S. C. Cartmell *et al.*, Multimodal characterization of the human nucleus accumbens. *Neuroimage* **198**, 137–149 (2019).
49. W. Cai, S. Ryali, T. Chen, C. S. R. Li, V. Menon, Dissociable roles of right inferior frontal cortex and anterior insula in inhibitory control: Evidence from intrinsic and task-related functional parcellation, connectivity, and response profile analyses across multiple datasets. *J. Neurosci.* **34**, 14652–14667 (2014).
50. M. X. Cohen, J. C. Schoene-Bake, C. E. Elger, B. Weber, Connectivity-based segregation of the human striatum predicts personality characteristics. *Nat. Neurosci.* **12**, 32–34 (2009).
51. W. van den Bos, C. A. Rodriguez, J. B. Schweitzer, S. M. McClure, Connectivity strength of dissociable striatal tracts predict individual differences in temporal discounting. *J. Neurosci.* **34**, 10298–10310 (2014).
52. K. H. MacNiven, J. K. Leong, B. Knutson, Medial forebrain bundle structure is linked to human impulsivity. *Sci. Adv.* **6**, 1–9 (2020).
53. J. W. Dalley, K. D. Ersche, Neural circuitry and mechanisms of waiting impulsivity: Relevance to addiction. *Philos. Trans. R. Soc. Lond. B Biol. Sci.* **374**, 20180145 (2019).
54. K. D. Ersche *et al.*, Abnormal brain structure implicated in stimulant drug addiction. *Science (80-.)* **335**, 601–604 (2012).
55. J. D. Yeatman, R. F. Dougherty, N. J. Myall, B. A. Wandell, H. M. Feldman, Tract profiles of white matter properties: Automating fiber-tract quantification. *PLoS One* **7**, e49790 (2012).
56. F. C. Yeh *et al.*, Quantifying differences and similarities in whole-brain white matter architecture using local connectome fingerprints. *PLOS Comput. Biol.* **12**, e1005203 (2016).
57. T. Nichols, A. Holmes, Nonparametric permutation tests for functional neuroimaging. *Hum. Brain Funct. Second Ed.* **25**, 887–910 (2003).
58. J. H. Patton, M. S. Stanford, E. S. Barratt, Factor structure of the Barratt impulsiveness scale. *J. Clin. Psychol.* **51**, 768–774 (1995).
59. K. N. Kirby, N. N. Maraković, Delay-discounting probabilistic rewards: Rates decrease as amounts increase. *Psychon. Bull. Rev.* **3**, 100–104 (1996).
60. D. D. Brewer, R. F. Catalano, K. Haggerty, R. R. Gainey, C. B. Fleming, A meta-analysis of predictors of continued drug use during and after treatment for opiate addiction. *Addiction* **93**, 73–92 (1998).
61. R. Kornfield, C. L. Toma, D. V. Shah, T. J. Moon, D. H. Gustafson, What do you say before you relapse? How language use in a peer-to-peer online discussion forum predicts risky drinking among those in recovery. *Health Commun.* **33**, 1184–1193 (2018).
62. J. D. Robinson *et al.*, Evaluating the temporal relationships between withdrawal symptoms and smoking relapse. *Psychol. Addict. Behav.* **33**, 105–116 (2019).
63. S. Steegen, F. Tuerlinckx, A. Gelman, W. Vanpaemel, Increasing transparency through a multiverse analysis. *Perspect. Psychol. Sci.* **11**, 702–712 (2016).
64. N. H. Naqvi, D. Rudrauf, H. Damasio, A. Bechara, Damage to the insula disrupts addiction to cigarette smoking. *Science (80-.)* **315**, 531–534 (2007).
65. A. D. B. Craig, How do you feel–now? The anterior insula and human awareness. *Nat. Rev. Neurosci.* **10**, 59–70 (2009).
66. B. J. Everitt *et al.*, Review. Neural mechanisms underlying the vulnerability to develop compulsive drug-seeking habits and addiction. *Philos. Trans. R. Soc. Lond. B Biol. Sci.* **363**, 3125–3135 (2008).
67. D. Belin, A. C. Mar, J. W. Dalley, T. W. Robbins, B. J. Everitt, High impulsivity predicts the switch to compulsive cocaine-taking. *Science (80-.)* **320**, 1352–1355 (2008).
68. J. Kruper *et al.*, Evaluating the reliability of human brain white matter tractometry. *bioRxiv*, 2021.02.24.432740 (2021).
69. D. D. Joshi *et al.*, The anterior insular cortex in the rat exerts an inhibitory influence over the loss of control of heroin intake and subsequent propensity to relapse. *Eur. J. Neurosci.* **52**, 4115–4126 (2020).
70. Z. F. H. Cao, D. Burdakov, Z. Sarnyai, Optogenetics: Potentials for addiction research. *Addict. Biol.* **16**, 519–531 (2011).
71. S. W. Yip, D. Scheinost, M. N. Potenza, K. M. Carroll, Connectome-based prediction of cocaine abstinence. *Am. J. Psychiatry* **176**, 156–164 (2019).
72. O. Hassan, S. Phan, N. Wiecks, C. Joaquin, V. Bondarenko, Outcomes of deep brain stimulation surgery for substance use disorder: A systematic review. *Neurosurg. Rev.* **44**, 1967–1976 (2021).
73. American Psychiatric Association, *Diagnostic and Statistical Manual of Mental Disorders (DSM-5)* (American Psychiatric Association, ed. 5, 2013).
74. S. D. Gosling, P. J. Rentfrow, W. B. Swann, A very brief measure of the Big-Five personality domains. *J. Res. Pers.* **37**, 504–528 (2003).
75. C. S. Carver, T. L. White, Behavioral inhibition, behavioral activation, and affective responses to impending reward and punishment: The BIS/BAS Scales. *J. Pers. Soc. Psychol.* **67**, 319–333 (1994).
76. A. T. Beck, C. H. Ward, M. Mendelson, J. Mock, J. Erbaugh, An inventory for measuring depression. *Arch. Gen. Psychiatry* **4**, 561–571 (1961).
77. L. C. Sobell, M. B. Sobell, "Timeline follow-back" in *Measuring Alcohol Consumption*, J. P. Allen, R. Z. Litten, Eds. (Humana Press, Totowa, NJ, 1992), pp. 41–72.
78. D. Hersh, C. L. Mulgrew, J. Van Kirk, H. R. Kranzler, The validity of self-reported cocaine use in two groups of cocaine abusers. *J. Consult. Clin. Psychol.* **67**, 37–42 (1999).
79. J. S. Cacciola *et al.*, Development and initial evaluation of the Brief Addiction Monitor (BAM). *J. Subst. Abuse Treat.* **44**, 256–263 (2013).
80. S. Mackey *et al.*; ENIGMA Addiction Working Group, Mega-analysis of gray matter volume in substance dependence: General and substance-specific regional effects. *Am. J. Psychiatry* **176**, 119–128 (2019).
81. S. Tolomeo, R. Yu, Brain network dysfunctions in addiction: A meta-analysis of resting-state functional connectivity. *Transl. Psychiatry* **12**, 41 (2022).